REPORT DOCUMENTATION PAGE

Form Approved
OMB No. 0704-0188

The public reporting burden for this collection of information is estimated to average 1 hour per response, including the time for reviewing instructions, searching existing data sources, gathering and maintaining the data needed, and completing and reviewing the collection of information. Send comments regarding this burden estimate or any other aspect of this collection of information, including suggestions for reducing the burden, to Department of Defense, Washington Headquarters Services, Directorate for Information Operations and Reports (0704-0188), 1215 Jefferson Davis Highway, Suite 1204, Arlington, VA 22202-4302. Respondents should be aware that notwithstanding any other provision of law, no person shall be subject to any penalty for failing to comply with a collection of information if it does not display a currently valid OMB control number.

PLEASE DO NOT RETURN YOUR FORM TO THE ABOVE ADDRESS.

1. REPORT DATE *(DD-MM-YYYY)*	2. REPORT TYPE	3. DATES COVERED *(From - To)*
10/10/2012	Final Performance Report	4/1/2010 - 3/31/2012

4. TITLE AND SUBTITLE

New Types of Artificial Muscles for Large Stroke and High Force Applications

5a. CONTRACT NUMBER

FA9550-09-1-0537

5b. GRANT NUMBER

FA9550-09-1-0537

5c. PROGRAM ELEMENT NUMBER

6. AUTHOR(S)

Ray H. Baughman and Mikhail E. Kozlov

5d. PROJECT NUMBER

5e. TASK NUMBER

5f. WORK UNIT NUMBER

7. PERFORMING ORGANIZATION NAME(S) AND ADDRESS(ES)

The University of Texas at Dallas
800 West Campbell Road
Richardson, TX 75080

8. PERFORMING ORGANIZATION REPORT NUMBER

UT Dallas 32655018

9. SPONSORING/MONITORING AGENCY NAME(S) AND ADDRESS(ES)

Byung-Lip Lee
AFOSR
4015 Wilson Boulevard, AFOSR/NA, Room 713
Arlington, VA 22203-1954

10. SPONSOR/MONITOR'S ACRONYM(S)

Byung-Lip Lee

11. SPONSOR/MONITOR'S REPORT NUMBER(S)

AFRL-OSR-VA-TR-2012-1188

12. DISTRIBUTION/AVAILABILITY STATEMENT

Distribution A: Approved for Public Release

13. SUPPLEMENTARY NOTES

14. ABSTRACT

This three-year AFOSR sponsored project resulted in discovery of four fundamentally new types of artificial muscles, advancement of technology for carbon nanotube yarn spinning that is needed for muscle fabrication, and has enabled studies in closely related areas such as sound generation in air and water. New types of muscles were designed using carbon nanotube and graphene assemblies available from the University of Texas at Dallas and include Aerogel Muscles, Torsional and Tensile Yarn Muscles, Artificial Muscles Based on Polypyrrole Laminates and Graphene-based muscles. The studies were published in 14 high impact papers including three papers in Science magazine, two patent filings, highlighted in numerous news media articles and in TV shows. The new muscles might be deployed for such diverse applications as morphing air vehicles, autonomous robots, and intelligent aircraft surfaces.

15. SUBJECT TERMS

Artificial Muscles, Actuators, Carbon Nanotubes

16. SECURITY CLASSIFICATION OF:			17. LIMITATION OF ABSTRACT	18. NUMBER OF PAGES	19a. NAME OF RESPONSIBLE PERSON
a. REPORT	b. ABSTRACT	c. THIS PAGE			19b. TELEPHONE NUMBER *(Include area code)*

Reset

Standard Form 298 (Rev. 8/98)
Prescribed by ANSI Std. Z39.18

TABLE OF CONTENTS

1. Executive Summary

This three-year AFOSR sponsored project resulted in discovery of several fundamentally new types of artificial muscles, development of technologies for upscaling carbon nanotube yarn spinning needed for muscle fabrication and enabled studies in closely related areas such as sound generation in air and water. The studies were published in 14 high impact papers, including three papers in *Science* magazine, two patent filings, and highlighted in numerous press releases and TV programs. As we reported in *Science* 2009, carbon nanotube aerogel sheets are the sole component of **new artificial muscles** that provide giant elongations and elongation rates of 220% and (3.7×10^4)% per second, respectively, at operating temperatures from 80 to 1900 K. These solid-state–fabricated sheets are enthalpic rubbers having gas-like density and specific strength in one direction higher than those of steel plate. Actuation of the sheets can be used for optimizing nanotube electrodes for organic light-emitting displays, solar cells, charge stripping from ion beams, and cold electron field emission. The **second new type** of artificial muscles is an electrolyte-filled twist-spun carbon nanotube yarn, much thinner than a human hair, which functions as a torsional artificial muscle in a simple three-electrode electrochemical system, providing a reversible 15,000° rotation and 590 revolutions per minute (*Science* 2011). The use of a torsional yarn muscle as a mixer for a fluidic chip was demonstrated. This work was extended to dry electrically, chemically, and photonically powered torsional and tensile hybrid carbon nanotube yarn muscles, submitted to *Science* in 2012. These twist-spun carbon nanotube yarns have useful topological complexity of electrolyte-free muscles that provide fast, high-force, large-stroke torsional and tensile actuation. Over a million reversible torsional and tensile actuation cycles are demonstrated, wherein a muscle spins a rotor at an average 11,500 revolutions/minute or delivers 3% tensile contraction at 1,200 cycles/minute. This rotation rate is 20 times higher than previously demonstrated for an artificial muscle and the 27.9 kW/kg power density during muscle contraction is 85 times higher than for natural skeletal muscle. **Another novel type of muscles** was prepared from highly anisotropic CNT sheets that were drawn from a carbon nanotube forest and periodically electrochemically laminated with polypyrrole (PPy) (*Advanced Materials* 2011). These muscles demonstrated significant improvement in actuation performance, with higher actuator strains in the transverse direction than for neat PPy. Prepared structures might eventually enable important commercial applications of conductive polymers as artificial muscles. The **forth type of artificial muscles** developed in the project are based on graphene and its derivatives. We found that graphene oxide nanoribbon mats exhibit up to 1.6% reversible contraction when electrically heated at ambient conditions, *Chemical Physics Letters* 2011. The experimentally derived work capacity of the mats

was about 40 J/kg, which is similar to that of natural muscle. In another study electromechanical actuators were fabricated using flexible graphene-based paper, and the stroke of these actuators was directly measured in response to an applied potential of –1 V in 1 M NaCl solution (*Advanced Functional Materials* 2011). Actuation strain up to 0.064% and 0.1% was obtained for pristine graphene and paper loaded with Fe_3O_4 nanoparticles, respectively. It was found that Fe_3O_4 nanoparticles partially prevent graphene sheets from restacking and allow the electrolyte ions to infiltrate the resulting magnetic graphene paper.

The need for incorporating functional guests in yarns led to development of **biscrolling technology** (*Science* 2011) that provided generically applicable methods for producing weavable yarns comprising up to 95 weight percent of otherwise unspinnable particulate or nanofiber powders that remain highly functional. This technology enables yarn weaving, sewing, knotting, braiding, and charge collection. Also towards the goal of providing a continuous process for the solid-state fabrication of carbon nanotube sheets and yarns from carbon nanotube forests, we developed the growth of yarn-spinnable and sheet-drawable carbon nanotube forests on highly flexible stainless steel sheets, instead of the conventionally used silicon wafers (*Carbon* 2010).

Finally remarkable performance of solid-state fabricated carbon nanotube sheets developed through program funding enabled such important applications as thermoacoustic projectors (*Nano Letters* 2010), sonars and photo-deflectors and for switchable invisibility cloaks (*Nanotechnology* 2011). Visibility cloaking was demonstrated in a liquid.

Success in accomplishing the main goal of the project added four fundamentally new types of artificial muscles to the arsenal of actuators that can be exploited for various DoD and civilian applications. The new actuator types could be deployed for such diverse DoD needs as morphing microair vehicles or larger aircraft, autonomous robots, and intelligent aircraft surfaces. Extensive teaming with collaborating researchers in US and abroad helped us to solve scientific and technological problems, and provided a path towards novel applications.

Another output of the program is two provisional patent filings in the United States on new technologies and devices developed in the course of this project.

2. Giant-Stroke, Superelastic Carbon Nanotube Aerogel Muscles

Improved electrically powered artificial muscles are needed for generating force, moving objects, and accomplishing work. Carbon nanotube aerogel sheets are the sole component of new artificial muscles [1] that provide giant elongations and elongation rates of 220% and (3.7×10^4)% per second, respectively, at operating temperatures from 80 to 1900 K (Figure 1). These solid-state–fabricated sheets are enthalpic rubbers having gas-like density and specific strength in one direction higher than those of steel plate. Actuation decreases nanotube aerogel density and can be permanently frozen for such device applications as transparent electrodes. Poisson's ratios reach 15, a factor of 30 higher than for conventional rubbers. These giant Poisson's ratios explain the observed opposite sign of width and length actuation and result in rare properties: negative linear compressibility and stretch densification.

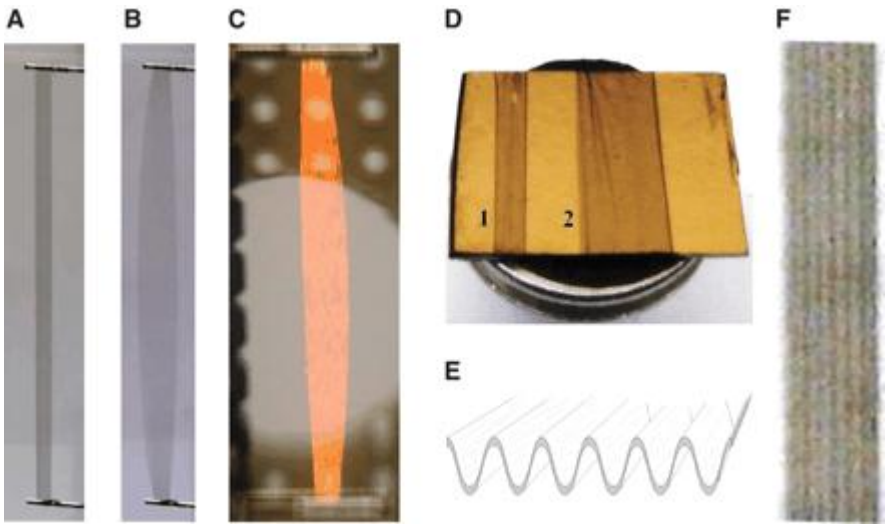

Figure. 1. (**A** and **B**) Photograph of a rigidly end-supported 50-mm-long by 2-mm-wide nanotube sheet strip (A) and the same sheet strip expanded in width by applying 5 kV with respect to ground (B). (**C**) Photograph of a 25-mm-long nanotube sheet strip actuated at 1500 K by applying 3 kV, where the color of incandescence is not correctly captured by the camera. (**D**) Picture of identical-dimension nanotube sheet strips of (A) and (B) that were contacted with a Au-coated Si substrate while in un-actuated (1) and actuated (2) states and subsequently densified on the substrate by absorption and evaporation of ethanol. (**E** and **F**) Schematic representation (E) and optical micrograph (F), taken at ~45° to the sheet-width direction to enhance visibility, of the periodic corrugation in the width direction that results from periodic cycling under the inhomogeneous strains caused by sheet strip ballooning.

In addition to extending the capabilities of artificial muscles to giant strokes and strain rates at extreme temperatures, present actuators provide other application possibilities that relate to the structural change of the nanotube sheets during large-stroke actuation. The nanotubes diffract light perpendicular to the alignment direction, which can be dynamically modulated at over kilohertz frequencies for optical applications. The ability to tune the density of nanotube sheets and then freeze this actuation is being used for optimizing nanotube electrodes for organic light-emitting displays, solar cells, charge stripping from ion beams, and cold electron field emission.

The work on aerogel muscles stimulated development of novel reel-wound carbon nanotube polarizers for terahertz frequencies. Using highly oriented multiwalled carbon nanotube aerogel sheets, we fabricated micrometer-thick freestanding carbon nanotube (CNT) polarizers. Simple winding of nanotube sheets on a U-shaped polyethylene reel (Figure 2) enabled rapid and reliable polarizer fabrication, bypassing lithographic or chemical etching processes. With the remarkable extinction ratio reaching ~37 dB in the broad spectral range from 0.1 to 2.0 THz, combined with the extraordinary gravimetric mechanical strength of CNTs, and the dispersionless character of freestanding sheets, the commercialization prospects for the authors' CNT terahertz polarizers appear attractive.

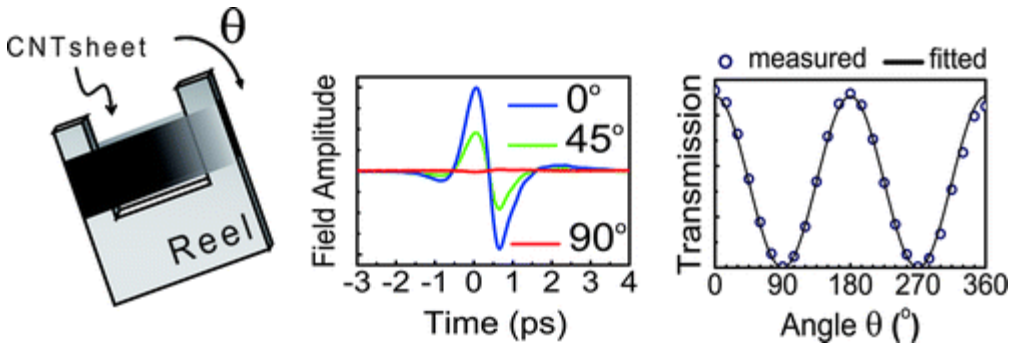

Figure 2. (a) Experimental scheme for the polarization state measurements. The incident THz beam is polarized along the *x*-axis and the CNT sheet polarizer was rotated from 0 to 360° degrees in 15° degree intervals. The 75-layer CNT sheet is used as a polarizer and 0° (90°) corresponds to the nanotube orientation direction being perpendicular (parallel) to the polarization of the incident THz waves. (b) Time traces for *x*-component (E_x) electric fields for the different polarizer angles (0, 45, and 90°). The reference signal (gray line) is measured without any CNT polarizer. More than two orders of magnitude extinction are observed between the perpendicular (0°) and parallel (90°) orientation.

3. Torsional and Tensile Carbon Nanotube Yarn Muscles

Rotary motors of conventional design can be rather complex and are therefore difficult to miniaturize; previous carbon nanotube artificial muscles provide contraction and bending, but not rotation. We show that an electrolyte-filled twist-spun carbon nanotube yarn, much thinner than a human hair, functions as a torsional artificial muscle in a simple three-electrode electrochemical system, providing a reversible 15,000° rotation and 590 revolutions per minute. A hydrostatic actuation mechanism, as seen in muscular hydrostats in nature (Figure 3) explains the simultaneous occurrence of lengthwise contraction and torsional rotation during the yarn volume increase caused by electrochemical double-layer charge injection. The use of a torsional yarn muscle as a mixer for a fluidic chip was demonstrated.

The combination of mechanical simplicity, large torsional rotation, high rotation rate, and micrometer-size yarn diameter suggests applications such as microfluidic pumps, valve drives, and mixers. We demonstrated one such application by using a carbon nanotube yarn torsional actuator to mix two laminarly flowing liquids (dyed yellow and blue) that were joined at a T-junction in a fluidic circuit (Figure 4). By switching between modest interelectrode potentials (0 V and –3 V at 1 Hz), we achieved a reversible paddle rotation of up to 180° with a 65-mm length of actuating yarn 15 μm in diameter. The yarn rotated a paddle that was 100 times the diameter of the yarn, and 80 times its mass, in the flowing liquids at a maximum rotation rate of 360°/s.

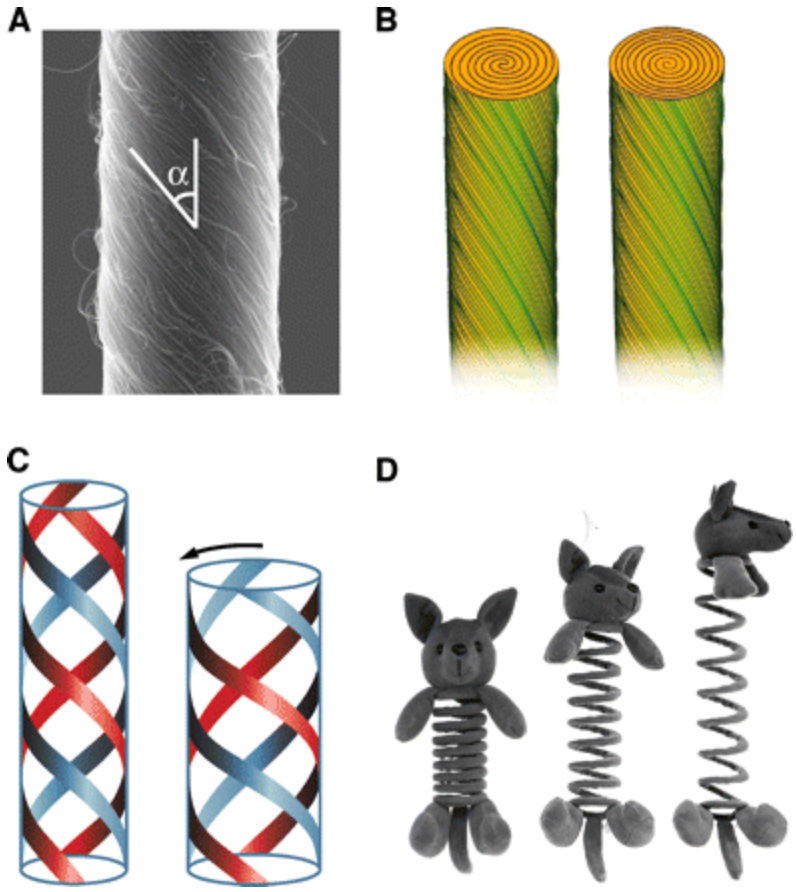

Figure 3. (**A**) Scanning electron micrograph of a carbon nanotube yarn (d = 3.8 μm, α = 37°) that was symmetrically twist-spun from a MWNT forest. (**B**) Schematic illustration of idealized Fermat (left) and Archimedean (right) scroll structures spun symmetrically and highly asymmetrically, respectively, from a carbon nanotube forest. (**C**) Schematic illustration of the effect of yarn volume expansion during charge injection on yarn length, yarn diameter, and yarn twist, where the pictures on left and right are before and after volume increase, respectively, and the ribbon lengths are approximately constant. The amount of yarn untwist during yarn volume expansion is indicated by the arrow. (**D**) Photographs of "Springa-Roo" child's toy showing that spring stretch causes spring twist to increase, which is opposite to the effect of stretch on the carbon nanotube yarns investigated here.

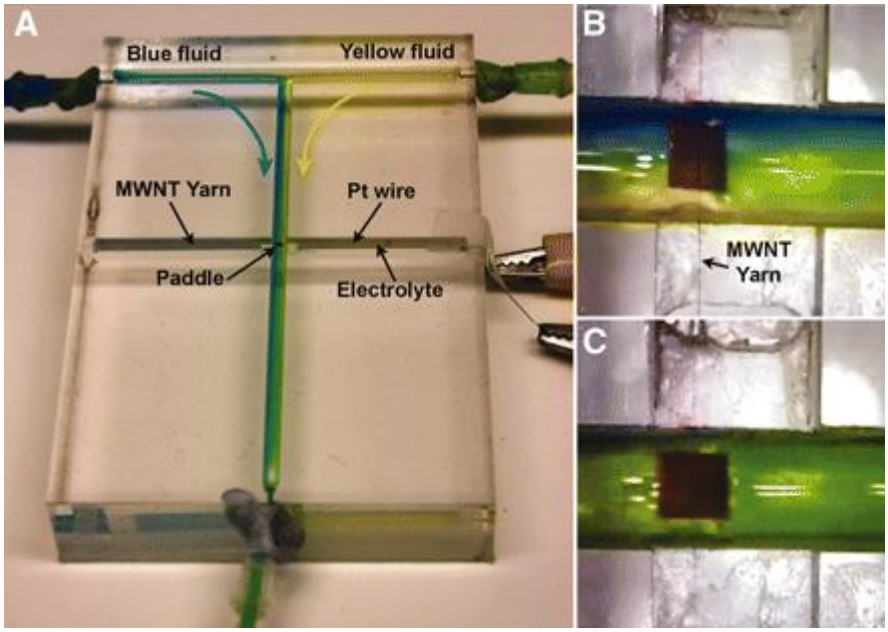

Figure 4. (**A**) Photograph of prototype mixer that can be downscaled for a microfluidic circuit. The channels are 3 mm wide. Mixing of water colored by blue and yellow food dye was by a paddle attached to the middle of a single piece of MWNT yarn that was half-immersed (cross channel on left) in electrolyte and torsionally actuated in opposite directions by alternately applying 0 V and –3 V between the yarn electrode and a Pt wire counter-electrode at 1 Hz. (**B** and **C**) Still images from movie showing unmixed food dye with mixer off (B) and the initial stage of mixing achieved when the mixer was first turned on (C). The electrolyte was 0.2 M TBA.PF_6 in acetonitrile.

On the macroscale, the demonstrated torsional actuation is well suited for rotating electrodes used in highly sensitive electrochemical analyte analysis, thereby eliminating the need for an ordinary motor. The torsional muscles can also be driven in reverse for conversion of mechanical energy to electrical energy, such as for sensors that generate electrical signals indicating applied mechanical torque or torsional rotation angle. The built-in linear-to-rotational coupling, voltage control, large and fast rotations, and easily handled yarn configuration suggest ready implementation for applications that require rotational positioning and high torque generation.

We extended this work in our recent study of electrically, chemically, and photonically powered torsional and tensile actuation of hybrid carbon nanotube yarn muscles. We have designed guest-filled, twist-spun carbon nanotube yarns having useful topological complexity (Figure 5) as electrolyte-free muscles that provide fast, high- force, large-stroke torsional and tensile actuation. Over a million reversible torsional and tensile actuation cycles are demonstrated, wherein a muscle spins a rotor at an average 11,500 revolutions/minute or delivers 3% tensile contraction at 1,200 cycles/minute. This rotation rate is 20 times higher than previously demonstrated for an artificial muscle and the 27.9 kW/kg power density during muscle contraction is 85 times higher than for natural skeletal muscle. Actuation of hybrid yarns by electrically, chemically, and photonically powered dimensional changes of yarn guest generates torsional rotation and contraction of the helical yarn host. Demonstrations include torsional motors, contractile muscles, and sensors that capture the energy of the sensing process to mechanically actuate.

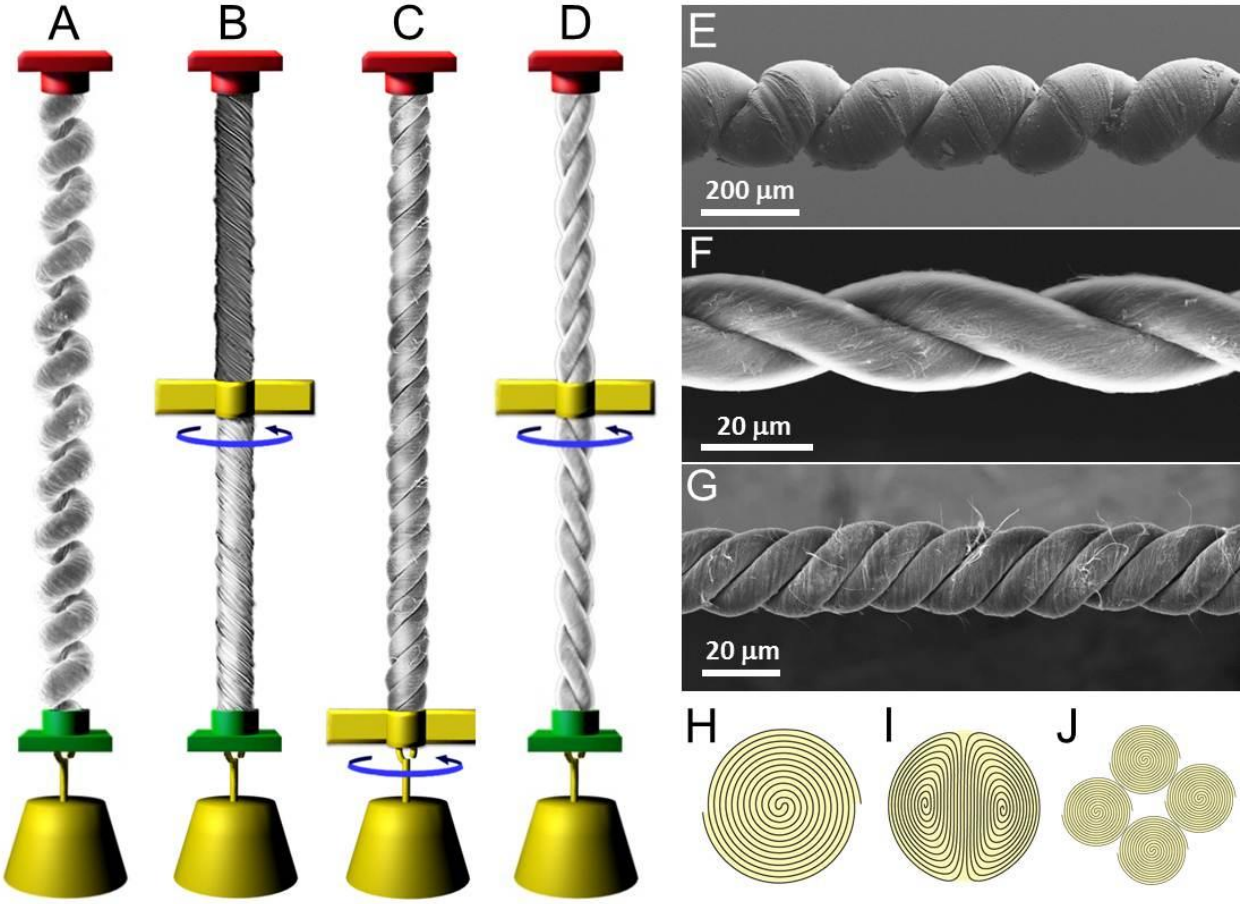

Figure 5**.** Muscle configurations and yarn structures for tensile and torsional actuation. (**A**-**D**) Tensile load and optional paddle positions for a two-end-tethered, fully-infiltrated homochiral yarn (A); a two-end-tethered, bottom-half-infiltrated homochiral yarn (B); a one-end-tethered, fully-infiltrated homochiral yarn (C); and a two-end-tethered, fully-infiltrated heterochiral yarn (D). The depicted yarns are coiled, non-coiled, four-ply, and two-ply, respectively. The arrows indicate the observed direction of paddle rotation during thermal actuation. Red and green yarn end attachments are tethers, meaning they prohibit end rotation – red attachments also prohibit translational displacement. (**E-G)** SEM micrographs of fully-infiltrated homochiral coiled yarn (E), neat two-ply yarn (F) and neat four-ply yarn (G). (**H**-**J**) Illustration of ideal cross-sections for Fermat (H), dual-Archimedean (I), and infiltrated four-ply Fermat yarns (J).

The realized tensile strokes and power densities for contraction are so high for coiled wax hybrid yarns that practical applications are expected for these high-cycle-life muscles. The major competing NiTi shape memory metal actuators have a highly hysteretic actuator stroke - control of actuator displacement is greatly complicated by the dependence of actuation on prior history within a cycle. This history dependence is small for the wax hybrid yarn, and should be negligible for cycling a neat yarn or any wax-filled yarn between molten states. While shape memory metals have been exploited as torsional actuators, the torsional actuation (0.15°/mm) is much smaller than demonstrated here for wax hybrid and PDA hybrid yarns (80 and 100°/mm, respectively). Improved control and large rotational actuation, along with potentially longer cycle life, suggest the use of yarn actuators in medical devices, robots, and shutters, for which shape memory alloys are

currently employed, as well as extension to microvalves, mixers, smart phone lenses, positioners and even toys.

Hybrid CNT muscles may also find importance as intelligent sensors that detect environmental conditions and provide either a reversible or non-reversible tensile or rotary response (depending upon the design). The described reversibly-actuating hydrogen-sensing actuator is one possibility – likely more important, biologically functionalized guests in biscrolled yarns could respond to analytes for self-powered sensing and/or control purposes. Intelligent clothing can be designed to provide variable porosity, wherein expanding or contracting guest materials would alter yarn length and diameter to open or close textile pores, thereby increasing comfort or protection against chemical threats.

4. Artificial Muscles Based on Polypyrrole/Carbon Nanotube Laminates

A novel route for producing polypyrrole-based PPy-CNT composites has been demonstrated, where highly anisotropic CNT sheets are drawn from a carbon nanotube forest and periodically electrochemically laminated with PPy (*Advanced Materials* 2011). Electrical conductivity was similarly increased as was the film electrochemical activity. These improvements led to a significant improvement in actuator performance, with higher actuator strains in the transverse direction than for neat PPy. The higher strength and stiffness of the laminates resulted in significantly higher strains under load than the neat PPy and doubled work per cycle. Electrochemically accelerated mechanical creep was also dramatically decreased by forming PPy/CNT laminates. The demonstrated increases in actuator stroke, work per cycle, strength, electrical conductivity, and creep resistance, as a result of lamination with anisotropic CNT sheets, might well eventually enable important commercial applications of conductive polymers as artificial muscles. While uniaxial laminates were produced in this study, the process can be easily adapted to produce cross-ply laminates.

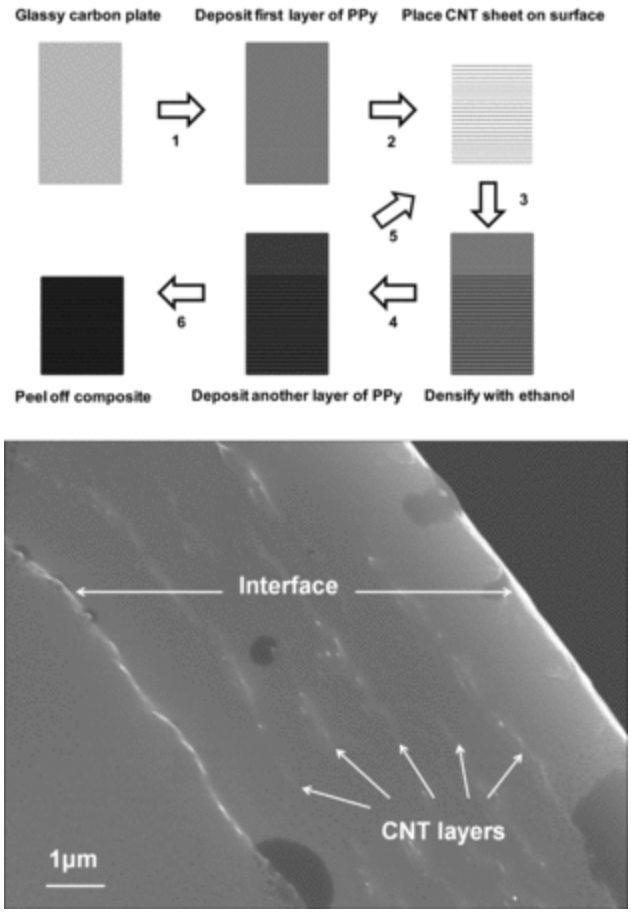

Figure 6. a) Schematic illustration of the sequential layering process used for forming PPy/CNT laminates; b) SEM image of a cross-section of a PPy/CNT laminate. The interfaces between the sample and the mounting epoxy are labeled.

5. Artificial Muscles Based on Graphene and Its Derivatives

In this study graphene oxide nanoribbons (GOr) were prepared by chemical unzipping of multi-walled carbon nanotubes and assembled into macroscopic mats by a vacuum filtration process. The prepared material exhibited unexpectedly large reversible contraction when heated with electrical current at ambient conditions. Exposure to water vapors resulted in the reversible expansion. The thermally-driven GOr actuators exhibited high work capacity (about 40 J/kg, Figure 7), which was limited by low mechanical strength of the material. The dimensional changes were associated with the adsorption/desorption of water molecules by the highly hydrophilic graphene oxide nanoribbons. It is expected that the alignment of nanoribbons in the sample and the increase of the mat strength can substantially increase both generated strain and work capacity. After optimization, GOr mats may challenge performance of powerful SMA actuators. The electrolyte-free thermally-driven GOr actuators can be used in the design of advanced artificial muscle systems.

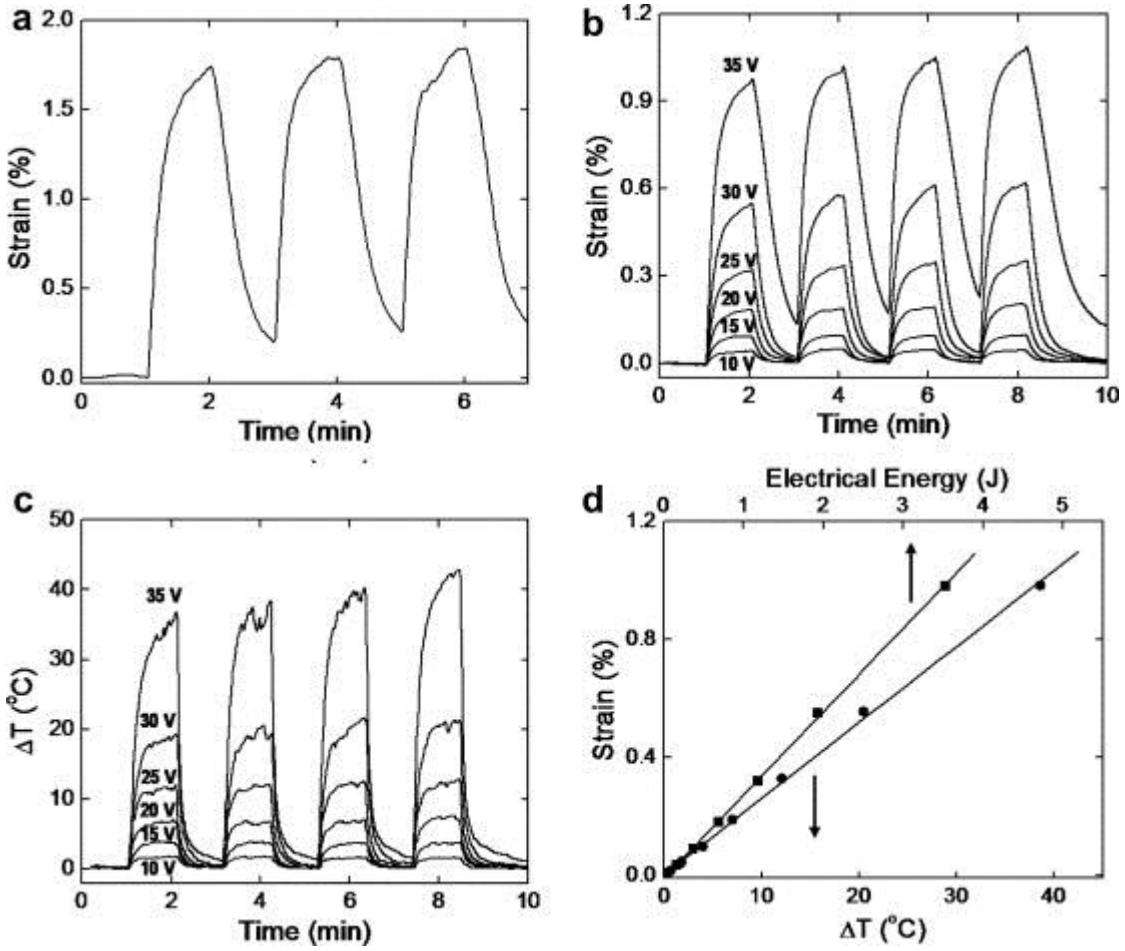

Figure 7. (a) Strain generated by GOr mat subjected to square wave voltage of 0–25 V at 2 minute period (b, c) strain and temperature profiles for another GOr mat subjected to square wave voltages of variable amplitudes. (d) Strain generated by GOr mat vs. supplied electrical energy (squares) and mat temperature (circles). Fit to experimental data is shown with straight lines. Positive strain corresponds to sample contraction. The data in (b, c, d) were recorded for the same sample.

Exceptionally high specific surface area, mechanical strength, electrical conductivity, and a special two-dimensional structure make graphene a highly promising material for electromechanical actuators. Electromechanical actuators are fabricated using flexible graphene-based paper prepared via a filtration process, Figure 8, and the stroke of these graphene-based actuators is directly measured during electrochemical double-layer charge injection (*Advanced Functional Materials* **21**, 3778-3784 (2011)) . Actuation strain up to 0.064% was obtained for pristine graphene paper in response to an applied potential of –1 V in 1 M NaCl solution. Double-layer charge injection in graphene sheets is believed to induce actuation strain through a combination of coulombic and quantum-chemical-based expansion. To increase electrochemical-double-layer capacitance and actuator performance, Fe_3O_4 nanoparticles were used to partially prevent graphene sheets from restacking and allow the electrolyte ions to infiltrate the resulting magnetic graphene paper more easily. The magnetic graphene paper exhibits actuation strain as large as 0.1% at –1 V applied potential, which is about 56% higher than that of the pristine graphene paper.

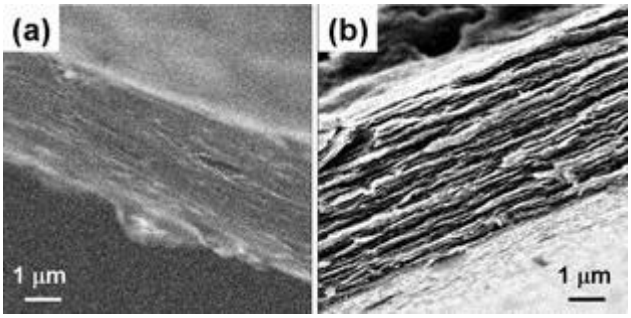

Figure 8**.** a) SEM image of the cross-section of PG-2 paper and b) MG-1 paper.

The roughly quadratic dependence of actuation strain on potential indicates that coulombic contribution to actuation dominates. However, higher strains are obtained for electron injection than for hole injection, which indicates that quantum-mechanically induced strains (which change sign with potential with respect to the potential of zero charge), and possibly volumetric effects that depend on solvated cation and solvated ion volumes, are important. By using experimental results and the surface area and area-normalized capacitance of single graphene sheets, we predict the dramatically increased actuator strokes that might be obtainable for graphene-flake structures in which sheet stacking does not occur.

6. Biscrolling and Other Enabling Technologies for Nanotube Muscles Fabrication

Multifunctional applications of textiles have been limited by the inability to spin important materials into yarns. Generically applicable methods are demonstrated [*Science* 2011) for producing weavable yarns comprising up to 95 weight percent of otherwise unspinnable particulate or nanofiber powders that remain highly functional. Scrolled 50-nanometer-thick carbon nanotube sheets confine these powders in the galleries of irregular scroll sacks whose observed complex structures are related to twist-dependent extension of Archimedean spirals, Fermat spirals, or spiral pairs into scrolls, Figure 9. The strength and electronic connectivity of a small weight fraction of scrolled carbon nanotube sheet enables yarn weaving, sewing, knotting, braiding, and charge collection. This technology is used to make yarns of superconductors, lithium-ion battery materials, graphene ribbons, catalytic nanofibers for fuel cells, and titanium dioxide for photocatalysis.

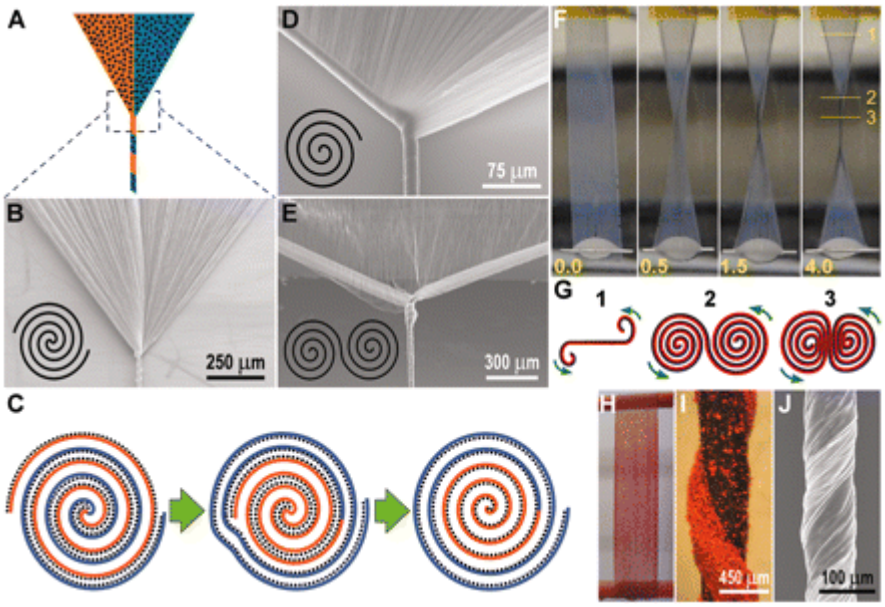

Figure 9. (**A**) Illustration of biscrolling by twist insertion in a spinning wedge, where black dots represent guest particles. (**B**) SEM micrograph of Fermat-type twist insertion during spinning from a MWNT forest. The inset illustrates a Fermat scroll. (**C**) Illustration of evolution from a Fermat scroll to an Archimedean scroll. (**D** and **E**) SEM images of guest-free spinning wedges showing Archimedean (D) and dual Archimedean (E) scrolls, which are illustrated in the insets. (**F**) Sequential photographs of liquid-state twist insertion in a 1-cm-wide MWNT sheet that is coated with filtration-deposited 92 wt % boron nitride nanotube guest. The number of inserted turns is shown at the bottom of each photograph. (**G**) Illustration of the expected cross sections at the positions marked in (F). (**H** and **I**) Photographs of a 1-cm-wide, bilayered stack fabricated by electrostatic deposition of a commercial red paint powder on a single MWNT sheet (H) and a biscrolled yarn made by dry-state twist insertion in a stack of eight MWNT sheets that was similarly electrostatically coated with this dry red paint (I) (*14*). (**J**) SEM image of a 70% Ti@$MWNT_{2,0}$ biscrolled yarn produced by symmetrically inserting twist in a rectangular bilayer sheet that is rigidly supported in a liquid bath. The Ti guest was deposited by electron beam evaporation.

A minute amount of MWNT host web enables twist-based spinning of yarn from diverse powders and nanofibers, while maintaining guest functionality. The mechanical properties of these webs enables weavability, knottability, and durability for biscrolled yarns containing up to at least 95 wt % guest, which can result in applications for wearable electronic textiles and for strong woven electrodes of batteries and fuel cells. Using patterned deposition for bilayer stacks, TiO_2 guest can be located in the sheath of a biscrolled yarn, thereby optimizing light absorption for such applications as self-cleaning textiles and Graetzel solar cells. The ability to make biscrolled yarns having Fermat, Archimedean, and dual Archimedean scroll geometries can be exploited to optimize yarn properties. The demonstrated use of CNT sheets as removable templates for making spinnable sheets of other nanotubes extends biscrolling to new hosts and provides a route to other types of nanotube yarns.

Towards the goal of providing a continuous process for the solid-state fabrication of carbon nanotube sheets and yarns from carbon nanotube forests, we reported the growth of yarn-spinnable and sheet-drawable carbon nanotube forests on highly flexible stainless steel sheets (SS), instead of

the conventionally used silicon wafers (*Carbon* 2010). Sheets and yarns were fabricated from the 16 cm maximum demonstrated forest width, from both sides of a stainless steel sheet, and the catalyst layer was shown to be reusable, thereby decreasing the need for catalyst renewal during a proposed continuous or semi-continuous process where the stainless steel sheet serves as a moving belt to enable forest growth at one belt end and carbon nanotube yarn or sheet fabrication at an opposite belt end, Figure 10.

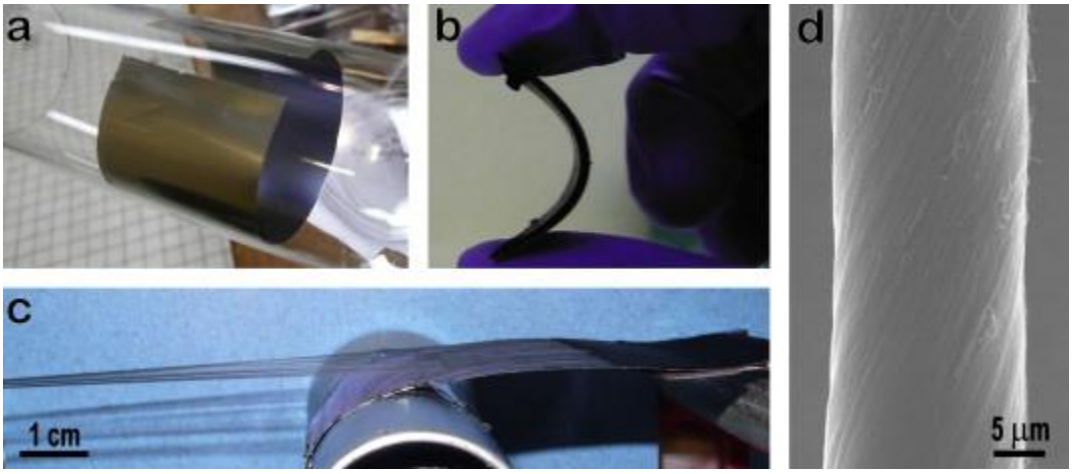

Figure 10. Flexibility of the SS substrate. Flexibility of the SS substrate before and after thermal CVD CNT forest growth: (a) a SS foil bent on the inner surface of the quartz tube (inner diameter, *ca.* 65 mm) used as a reactor chamber before to be submitted to the CVD thermal process. (b) Piece of a forest growth on a SS foil being elastically bent. (c) Photograph of a 5 cm wide CNT sheet being pulled from a forest growth on a bent SS substrate. (d) SEM image of a CNT yarn spun from a forest growth on SS.

The effects of processing conditions and apparent nanotube length on properties were investigated for carbon nanotube yarns obtained by solid-state drawing of an aerogel from a forest of multi-walled carbon nanotubes. Investigation of twist, false twist, liquid densification and combination methods for converting the drawn aerogel into dense yarn show that permanent twist is not needed for obtaining useful mechanical properties when nanotube lengths are long compared with nanotube diameters. Average mechanical strengths of 800 MPa were obtained for polymer-free twist-spun multi-walled carbon nanotube (MWNT) yarns and average mechanical strengths of 1040 MPa were obtained for MWNT yarns infiltrated with 10 wt% polystyrene solution. Strategies for increasing the mechanical properties are suggested based on analysis of intra-wall, intra-bundle and inter-bundle stress transfer.

7. Underwater Sound Generation and Mirage effect

The application of solid-state fabricated carbon nanotube sheets as thermoacoustic projectors is extended from air to underwater applications, thereby providing surprising results (*Nano Letters* 2010). While the acoustic generation efficiency of a liquid immersed nanotube sheet is profoundly degraded by nanotube wetting, the hydrophobicity of the nanotube sheets in water results in an air envelope about the nanotubes that increases pressure generation efficiency a hundred-fold over that obtained by immersion in wetting alcohols. Due to non-resonant sound generation, the emission spectrum of a liquid-immersed nanotube sheet varies smoothly over a wide

frequency range, 1-105 Hz. The sound projection efficiency of nanotube sheets substantially exceeds that of much heavier and thicker ferroelectric acoustic projectors in the important region below about 4 kHz, and this performance advantage increases with decreasing frequency. While increasing thickness by stacking sheets eventually degrades performance due to decreased ability to rapidly transform thermal energy to acoustic pulses, use of tandem stacking of sepd. nanotube sheets (that are addressed with phase delay) eliminates this problem. Encapsulating the nanotube sheet projectors in argon provided attractive performance at needed low frequencies, as well as a realized energy conversion efficiency in air of 0.2%, which can be enhanced by increasing the modulation of temperature.

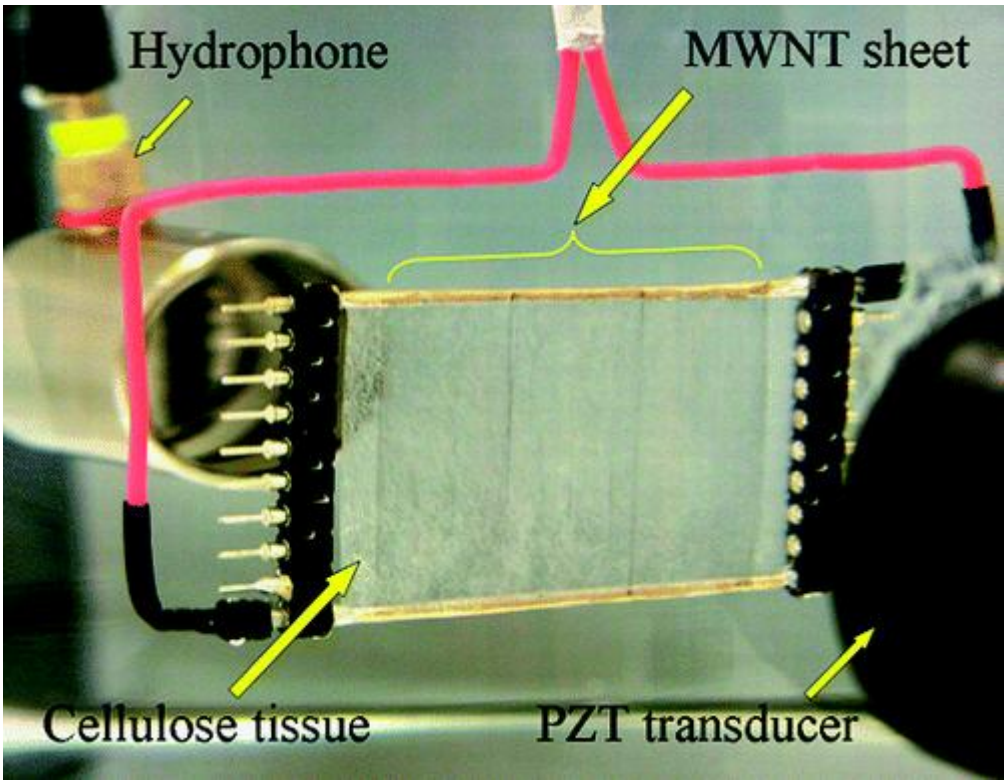

Figure 11. Carbon nanotube sheet used for underwater sound generation.

The single-beam mirage effect, also known as photothermal deflection, was studied using a free-standing, highly aligned carbon nanotube aerogel sheet as the heat source (*Nanotechnology* 2011). The extremely low thermal capacitance and high heat transfer ability of these transparent forest-drawn carbon nanotube sheets enables high frequency modulation of sheet temperature over an enormous temperature range, thereby providing a sharp, rapidly changing gradient of refractive index in the surrounding liquid or gas. The advantages of temperature modulation using carbon nanotube sheets are multiple: in inert gases the temperature can reach > 2500 K; the obtained frequency range for photothermal modulation is ~100 kHz in gases and over 100 Hz in high refractive index liquids; and the heat source is transparent for optical and acoustical waves. Unlike for conventional heat sources for photothermal deflection, the intensity and phase of the thermally modulated beam component linearly depends upon the beam-to-sheet separation over a wide range of distances. This aspect enables convenient measurements of accurate values for thermal diffusivity and the temperature dependence of refractive index for both liquids and gases. The remarkable

performance of nanotube sheets suggests possible applications as photo-deflectors and for switchable invisibility cloaks, and provides useful insights into their use as thermoacoustic projectors and sonar. Visibility cloaking is demonstrated in a liquid.

8. Project participants

Ray H. Baughman
Márcio D. Lima
Na Li
Mônica Jung de Andrade
Shaoli Fang
Jiyoung Oh
Mikhail E. Kozlov
Carter S. Haines
Dongseok Suh
Leonardo D. Machado
Ali Aliev

9. Publications

1. "Giant Stroke, Superelastic Carbon Nanotube Aerogel Muscles", A. E. Aliev, J. Oh, M. E. Kozlov, A. A. Kuznetsov, S. Fang, A. F. Fonseca, R. Ovalle, M. D. Lima, M. H. Haque, Y. N. Gartstein, M. Zhang, A. A. Zakhidov, R. H. Baughman, *Science* **323**, 1575-1578 (2009).

2. "Molecular, Supramolecular, and Macromolecular, Motors and Artificial Muscles", D. Li, Walter F. Paxton, R. H. Baughman, T. J. Huang, J. F. Stoddart, and P. S. Weiss, *MRS Bulletin* **34**, 671-681 (2009).

3. "Underwater Sound Generation Using Carbon Nanotube Projectors", A. E. Aliev, M. D. Lima, S. Fang, and R. H. Baughman, *Nano Letters* **10**, 2374-2380 (2010).

4. "Spinnable Carbon Nanotube Forests Grown on Thin, Flexible Metallic Substrates", X. Lepró, M. D. Lima, R. H. Baughman, *Carbon* **48**, 3621-3627 (2010).

5. "Structure and Process Dependent Properties of Solid-State Spun Carbon Nanotube Yarns", S. Fang, M. Zhang, A. A. Zakhidov, and R. H. Baughman, *Journal of Physics: Condensed Matter* **22**, 334221, 6 pp (2010).

6. "Nanofiber Actuators and Strain Amplifiers", A. E. Aliev, J. Oh, M. E. Kozlov, A. A. Kuznetsov, S. Fang, A. F. Fonseca, R. Ovalle, M. D. Lima, M. H. Haque, Y. N. Gartstein, M. Zhang, A. A. Zakhidov, R. H. Baughman, PCT International Appl. (2010), 2010019942 A2 20100218.

7. "Torsional Carbon Nanofiber Actuators and Methods to Make and Use Same", J. Foroughi, T. Mirfakhrai, G. M. Spinks, J. D. Madden, J. Oh, M. E. Kozlov, S. D. Fang, G. G. Wallace, R. H. Baughman, US Patent Appl. Serial No. 61/304,616 (Filed Feb. 15, 2010).

8. “Electromechanical Actuators Based on Graphene and Graphene/Fe_3O_4 Hybrid Paper”, J. Liang, Y. Huang, J. Oh, M. Kozlov, D. Sui, S. Fang, R. H. Baughman, Y. Ma, Y. Chen, *Advanced Functional Materials* **21**, 3778-3784 (2011).

9. ”Thermal Actuation of Graphene Oxide Nanoribbon Mats”, J. Oh, M. E. Kozlov, J. Carretero-González, E. Castillo-Martínez, and R. H. Baughman, *Chemical Physics Letters* **505**, 31–36 (2011).

10. “Artificial Muscles Based on Polypyrrole/Carbon Nanotube Laminates”, W. Zheng, J. M. Razal, P. G. Whitten, R. Ovalle-Robles, G. G. Wallace, R. H. Baughman, and G. M. Spinks, *Advanced Materials* **23**, 2966-2970 (2011).

11. "Mirage Effect from Thermally-Modulated Transparent Carbon Nanotube Sheet", A. E. Aliev, Y. N. Gartstein, R. H. Baughman, *Nanotechnology* **22**, 435704 (10 pp) (2011)

12. “Torsional Carbon Nanotube Artificial Muscles”, J. Foroughi, G. M. Spinks, G. G. Wallace, J. Oh, M. E. Kozlov, S. Fang, T. Mirfakhrai, J. D. W. Madden, M. K. Shin , S. J. Kim, and R. H. Baughman, *Science* **334**, 494-497 (2011).

13. “Biscrolling Nanotube Sheets and Functional Guests Into Yarns”, M. D. Lima, S. Fang, X. Lepró, C. Lewis, R. Ovalle-Robles, J. Carretero-González, E. Castillo-Martínez, M. E. Kozlov, J. Oh, N. Rawat, C. S. Haines, M. H. Haque, V. Aare, S. Stoughton, A. A. Zakhidov, R. H. Baughman, *Science*, **331**, 51-55 (2011).

14. “A Reel-Wound Carbon Nanotube Polarizer for Terahertz Frequencies”, J. Kyoung, E. Y. Jang, M. D. Lima, H. Park, R. Ovalle Robles,X. Lepró, Y. H. Kim, R. H. Baughman, D.-S. Kim, *Nano Letters* **11**, 4227-4231 (2011).

15. “Fabrication of Biscrolled Fiber Using Carbon Nanotube Sheet”, S. Fang, M. D. Lima, X. N. Lepro-Chávez, J. Carretero-González, E. Castillo-Martínez, R. Ovalle-Robles, C. S. Haines, D. M. Novitski, M. H. Haque, C. Lewis-Azad, M. E. Kozlov, A. A. Zakhidov, R. H. Baughman, Appl. Serial No. PCT/US2010/36378 (Filed May 27, 2010 and published January 13, 2011) PCT Patent WO2011005375 (A2).